Fabrication and Characterization of Biodegradable Poly(3-hydroxybutyrate) Composite Containing Bioglass

Superb K. Misra,[†] Showan N. Nazhat,[‡,§] Sabeel P. Valappil,[∥] M. Moshrefi-Torbati,[⊥] Robert J. K. Wood,[⊥] Ipsita Roy,[∥] and Aldo R. Boccaccini*[,†]

Department of Materials, Imperial College London, London SW7 2BP, United Kingdom, Division of Biomaterials and Tissue Engineering, Eastman Dental Institute, University College London, London WC1X 8LD, United Kingdom, Department of Molecular and Applied Biosciences, University of Westminster, London W1W 6UW, United Kingdom, and Research Institute for Industry, University of Southampton, Southampton SO17 1BJ, United Kingdom

Received February 16, 2007; Revised Manuscript Received April 5, 2007

Bacterially derived poly(3-hydroxybutyrate) (P(3HB)) has been used to produce composite films by incorporating Bioglass particles (<5 μm) in 5 and 20 wt % concentrations. P(3HB) was produced using a large scale fermentation technique. The polymer was extracted using the Soxhlet technique and was found to have similar thermal and structural properties to the commercially available P(3HB). The effects of adding Bioglass on the microstructure surface and thermal and mechanical properties were examined using differential scanning calorimetry, dynamic mechanical analysis (DMA), X-ray diffraction, surface interferometry, electron microscopy, and nanoindentation. The addition of increasing concentrations of Bioglass in the polymer matrix reduced the degree of crystallinity of the polymer as well as caused an increase in the glass transition temperature as determined by DMA. The presence of Bioglass particulates reduced the Young's modulus of the composite. The storage modulus and the loss modulus, however, increased with the addition of 20 wt % Bioglass. A short period (28 days) in vitro bioactivity study in simulated body fluid confirmed the bioactivity of the composites, demonstrated by the formation of hydroxyapatite crystals on the composites' surface.

1. Introduction

The availability of improved bone substitutes can lead to the cure of bone defects arising from trauma, tumor, or diseases.[1] Bone repair or regeneration has been a common, yet complicated, clinical problem in orthopedic surgery, and the use of autogenic and allogenic bones for treating bone defects is widely accepted.[2] In the latter case, however, the occurrence of immune related problems in the recipient's body has been reported, leading to infections and other health problems.[3] Tissue engineering (TE) has progressed in the last two decades to become a very promising alternative toward the repair of damaged tissues, in particular by avoiding the need for a permanent implant.[4−5] Numerous biocompatible materials are being investigated[4−7] to serve as scaffolds, e.g., support for cells in tissue engineering and tissue repair strategies. Among them, biodegradable polymers, both natural and synthetic, are especially considered due to their potential ability to enable cell adhesion, migration, proliferation, and differentiated function.[6−9]

Polymers of the polyhydroxyalkanoate (PHA) family are promising materials for biomedical applications due to their natural occurrence, proven biocompatibility, and tailorable bioabsorbability.[6] More than 100 different known types of PHAs with different structures have been reported.[10] Due to the variable composition of PHAs, a wide range of mechanical properties and degradation rates can be achieved.[11] P(3HB) is the simplest and most common member of the PHA family and has high potential for application as degradable TE scaffold.[12−14] It is a natural thermoplastic polymer produced by many types of microorganisms,[15] and it can be extracted as a stereoregular, optically active, isotactic polyester with high purity and without any inclusion of catalyst residues.[11] In addition to its biocompatibility and biodegradability, P(3HB) has been reported to have piezoelectric properties, which can stimulate bone growth and aid in healing.[16] The fact that low-molecular-weight P(3HB) occurs naturally in human blood,[17] and that its molecules decompose into 3-hydroxybutyric acid, provides further evidence of the biocompatibility and nontoxicity of this polymer. Previous studies have shown P(3HB) to have compatibility when in contact with various cells (fibroblasts, osteoblasts, endothelium cells, isolated hepatocytes).[18−21]

P(3HB), however, suffers from low strength and poor bioactivity (ability to form a direct chemical bond with surrounding bone tissue), which restricts its application in bone-tissue repair. To remediate this situation, composites of PHAs and bioactive ceramics are being developed to impart mechanical strength and bioactivity.[14,22−24] Doyle et al. carried out one of the first attempts of using bioceramic particles to reinforce PHAs in the early 1990s.[13] As reviewed elsewhere,[14,25] the composite concept is finding renewed impetus for production of improved bioactive scaffolds for tissue engineering.

Bioglass type 45S5 is a member of the family of bioactive glasses that elicit a specific physiological response, including the presence of surface-reactive silica, which leads to formation of a thin layer of carbonate hydroxyapatite (similar to biological apatite) on the glass surface when implanted or in contact with biological fluids in vitro and in vivo.[26−27] Through the hydroxyapatite surface layer, Bioglass, even if incorporated in biodegradable matrices, forms tenacious bonds to both hard and

* To whom correspondence should be addressed. E-mail: a.boccaccini@imperial.ac.uk.

[†] Imperial College London.

[‡] University College London.

[§] Current address: Department of Mining, Metals, and Materials Engineering, McGill University, Montreal, Canada H3A 2BZ.

[∥] University of Westminster.

[⊥] University of Southampton.

10.1021/bm0701954 CCC: $37.00 © 2007 American Chemical Society
Published on Web 05/27/2007

soft tissues when exposed to physiological fluids such as acellular simulated body fluid (SBF).[28] Moreover, it has been shown that bioactive glasses provide an ideal environment for cell colonization and proliferation and, in particular, dissolution products of 45S5 Bioglass can up-regulate diverse families of genes in osteoblast cells[29] and enhance differentiation of human osteoblasts to form new bone. Bioglass, being bioactive, biocompatible, osteoconductive, nontoxic, and noninflammatory, as well as being a nonimmunogenic agent, is very useful as filler in biopolymer composites as it can be used additionally to improve the mechanical properties of the composites as well as to influence its rate of degradation.[4,25,28,30]

This study investigated the fabrication of bioactive composites based on P(3HB) grown and extracted from *Bacillus cereus* SPV[31] and 45S5 Bioglass particulate inclusions. As a part of this study, first, the thermal properties of the extracted polymer were determined and compared with those of commercially available P(3HB) to evaluate the similarity of these two polymers. Second, bioactive composite films were fabricated using solvent casting technique, and they were characterized by means of standard analytical methods. Thermomechanical analysis of P(3HB) and P(3HB) composites with different concentration of Bioglass particles was carried out using dynamic mechanical analysis and differential scanning calorimetry. The combination of biodegradable P(3HB) and bioactive Bioglass enables the design of a new family of bioactive composites with potential applications in bone tissue engineering scaffolds.

2. Materials and Methods

2.1. P(3HB) Production and Extraction. All chemicals for polymer production were obtained from Sigma-Aldrich Company Ltd., (Dorset, England). For comparison purpose, commercial P(3HB) was purchased from Fluka Chemicals (Schnelldorf, Germany) and used without further purification.

P(3HB) samples were isolated from a newly characterized Gram positive bacteria *Bacillus cereus* SPV (obtained from the culture collection of University of Westminster, U.K.). The process has been described elsewhere;[31] hence, only the general description is given here. The fermentor was sterilized while containing only the salts of Kannan and Rehacek medium (Table 1)[32] and the pH adjusted to 6.8. The bacteria were grown in batch cultures in a 20 L fermentor for 72 h at 30 °C (impeller speed of 250 rpm, airflow rate at 1.0 vvm). The extraction of P(3HB) was carried out by the Soxhlet technique.[31] Briefly, the cells were harvested and lyophilized followed by a 16% sodium hypochlorite treatment at 37 °C for 1 h. The residue was washed twice each with water, acetone, ethanol, and diethyl ether[33]and, finally, subjected to Soxhlet extraction for 24 h using chloroform as the solvent. The chloroform containing P(3HB) was then concentrated by a vacuum rotary evaporator, and the P(3HB) was precipitated using 10 volumes of ice cold methanol. The dry cell mass obtained from the 20 L fermentor was 40 ± 5 g, with a polymer yield of 40%.

2.2. P(3HB) and P(3HB)/Bioglass Film Preparation. Solvent casting was carried out using analytical grade reagents procured from VWR International Ltd. (Poole, England). Neat polymer and composite films were prepared by solvent casting. Chloroform was used to dissolve P(3HB) using a polymer to solvent ratio of 3% (w/v).This polymer concentration was optimized on the basis of the homogeneity of the films produced (as discussed below). A melt-derived bioactive glass powder (Bioglass grade 45S5) with mean particle size <5 μm was used. The composition of the glass was as follows: 45 wt % SiO_2, 24.5 wt % Na_2O, 24.5 wt % CaO, and 6 wt % P_2O_5. Hench and co-workers first developed this composition in 1971, which has been extensively used in biomedical applications.[26−27] To prepare the composites, appropriate quantities of Bioglass powder were added to the polymer solution to yield composites with 5 and 20 wt % Bioglass concentration. The concentration of 5 wt % Bioglass was chosen on the basis of literature results[25] which have indicated this to be close to the optimal concentration of Bioglass in polymer matrices from the in-vitro biological point of view. The higher concentration (20 wt %) was chosen for comparison purposes and to gain new data on the composite behavior as the combination P(3HB)/Bioglass has not been studied before. The mixtures were then sonicated for 1 min (Ultrasonic Homogenizers US200, Philip Harris Scientific, Leicestershire, U.K.) to improve the dispersion of Bioglass particles by desegregating possible Bioglass particle agglomerations. The films were cast on glass petri dishes to achieve film thickness of the order of 100−200 μm. Once the films had been cast, they were washed with water and vacuum-dried for complete removal of the solvent. The films were stored in desiccators for further analysis.

2.3. P(3HB) Characterization. *2.3.1. Molecular Weight Measurements.* Molecular mass analysis was conducted by dissolving P(3HB) in chloroform. The solutions were heated at 50 °C and cooled before being filtered through 0.2 μm polyamide membrane. The GPC system was equipped with PLgel guard plus 2× mixed bed-B column (30 cm × 10 μm). The eluted polymer was detected with a differential refractometer. The data were collected and analyzed using Viscotek *Trisec 2000* and *Trisec 3.0* software. The GPC system was calibrated with polystyrene calibrants.

2.3.2. X-ray Diffraction. X-ray diffraction (XRD) analysis on the polymeric samples was performed using a Phillips PW1700 series automated powder diffractometer. Cu Kα radiation of 40 kV and 40 mA was obtained using a secondary crystal monochromator. The analytical parameters were the following: step size 0.04°, scan step time of 1 s, and diffraction range 5−55° (2θ).

2.3.3. Differential Scanning Calorimetry. Differential scanning calroimetry (DSC) measurements were performed with a Perkin-Elmer Pyris Diamond DSC (Perkin-Elmer Instruments). The sample masses for these measurements were in the range 4−6 mg. Samples were encapsulated in standard aluminum pans, and all tests were carried out under inert nitrogen. The samples were heated/cooled/heated at a heating rate of 20 °C min^{-1} between −50 and 200 °C.

2.3.4. Mechanical Tests. Tensile tests were carried out on sheets cut out from films (see section 2.3) with a width of 1.4 mm, length of 7−8 mm, and thickness in the range 140−200 μm. Nine repeat specimens were tested for this experiment. The tensile tests were carried out on a Perkin-Elmer dynamic mechanical analyzer at room temperature. The initial load was set to 1 mN, and it was increased to 6000 mN at a rate of 200 mN min^{-1}. The static modulus, stress, and strain were recorded during the measurement.

2.3.5. Dynamic Mechanical Analysis. Dynamic mechanical analysis (DMA) was carried out on polymeric films with a width of 3 mm and thickness in the range 140−200 μm as mentioned for static tests. Five repeat specimens were tested in tension under the stress control mode. The tests were carried out on a Perkin-Elmer dynamic mechanical analyzer (DMA 7e) apparatus. A temperature scan from −20 to 130 °C at a heating rate of 4 °C min^{-1} was applied. A frequency of 1 Hz was used, with a static tension control of 110% and a controlled dynamic strain of 0.2%. Nitrogen was used as purge. The viscoelastic parameters of storage modulus (E'), loss modulus (E''), and mechanical loss tangent (tan δ) were recorded as a function of temperature.

2.3.6. Nanoindentation. Nanoindentation tests were carried out to test the hardness of the composite films using a NanoTest (Micro Materials Ltd. U.K.) instrument. A loading rate of 0.01 mN/s was used. Films on the order of 80−120 μm in thickness were tested at room temperature. At least 15 indents were made in random locations on each film. The hardness of the composites was calculated by dividing the maximum load by the contact area.

2.4. P(3HB)/Bioglass Composite Characterization. Microstructural observations of P(3HB)/Bioglass composite samples were performed using a JEOL 5610LV scanning electron microscope (JEOL). The samples were placed on 8 mm diameter aluminum stubs. A gold sputtering device (EMITECH-K550) was used to coat the samples,

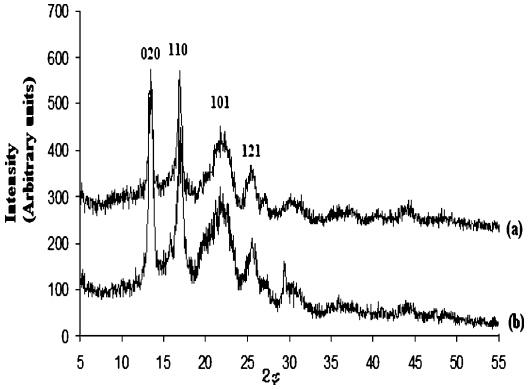

Figure 1. X-ray diffraction patterns of (a) commercially available P(3HB) and (b) lab grown P(3HB). Skrbic et al.[35] calculated unit cell parameters on the basis of the positions (2φ) of well separated diffraction maxima (020), (110), (101), and (121) using the quadratic form of the rhombic cell.

operating at a pressure of 7×10^{-2} bar and deposition current of 20 mA for 2 min. SEM images were taken at various acceleration voltages (max of 20 kV) to avoid beam damage on the polymer. White light interferometry was used to obtain 3D imaging of the surface topography of samples by means of the analyzer ZYGO (New View 200 OMP 0407C). These measurements allowed to investigate and quantify the roughness and topography of the surfaces. Differential scanning calorimetry, mechanical tests, DMA, and nanoindentation tests were carried out using the same equipment and conditions outlined in section 2.3.

2.5. Bioactivity Tests of P(3HB)/Bioglass Composites. In vitro bioactivity studies were carried out using acellular simulated body fluid (SBF), as developed by Kokubo et al.[34] The reagents were dissolved into HPLC (high performance liquid chromatography) grade water. The pH of SBF was adjusted to 7.25 at 37 °C using HCl. Samples with different wt % of Bioglass were immersed in SBF and maintained at 37 °C in an incubator. The SBF was refreshed after 48 h of incubation followed by every 3 days. Films were collected after 5, 7, and 28 days of incubation and washed with distilled water and vacuum-dried for 3 h before further examination. The *in vitro* degraded samples were then further characterized using SEM and XRD to determine the formation of hydroxyapatite on their surfaces.

3. Results

3.1. Polymer Characterization. The X-ray diffractograms of the extracted polymer indicated that there are no additional crystalline phases present when compared with a commercially available P(3HB), as shown in Figure 1.

The thermal properties of the extracted polymer were analyzed using DSC. Figure 2 shows DSC comparative plots of the commercial polymer with the lab grown polymer, while Table 1 presents a comparison of the thermal properties of both materials. The thermal measurements for both samples are quoted from the second heating run. The crystallization temperature and the glass transition temperature of these two polymers were found to be very similar. However, there was a slight decrease in the melting temperature for the lab grown polymer compared to the commercial P(3HB). The crystallinity percentage was determined by measuring the enthalpy of fusion from the differential scanning calorimetry curve, as shown in Figure 2, by using the following equation

$$\%\text{crystallinity}\ (X_c) = \frac{\Delta H_{f(\text{sample})}}{\Delta H_{f(100\%\text{crystalline})}} \times 100 \qquad (1)$$

where $\Delta H_{f(\text{sample})}$ is the enthalpy of fusion for the extracted P(3HB) sample and $\Delta H_{f(100\%\ \text{crystalline})}$ is the enthalpy of fusion

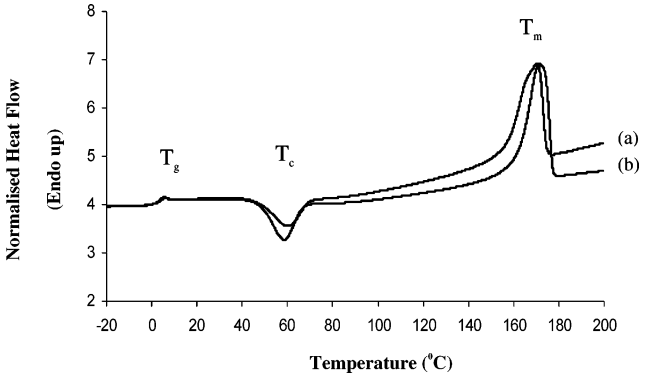

Figure 2. Normalized DSC heating curves of (a) lab grown P(3HB) and (b) commercial P(3HB) obtained at a heating rate of 20 °C min^{-1}. The curves have been shifted vertically for clarity [T_g = glass transition temperature, T_m = melting temperature, T_c = Crystallization temperature].

Table 1. Thermal Properties of Lab Grown P(3HB) Compared with Commercially Available P(3HB)[a]

properties	commercial P(3HB) powder	lab grown P(3HB) powder
T_m[b] (°C)	172.2 ± 0.6	169 ± 2
T_g[c] (°C)	2.0 ± 0.3	1.9 ± 0.2
T_c[d] (°C)	58.9 ± 0.5	59 ± 2
ΔH_f[e] (J/g)	70 ± 9	68.5 ± 0.3
X_c[f] (%)	0.47	0.46

[a] Data gathered from the second heating curve of DSC (see Figure 1b). [b] T_m = melting temperature. [c] T_g = glass transition temperature. [d] T_c = crystallization temperature. [e] ΔH_f = heat of fusion. [f] X_c = degree of crystallinity.

for a 100% crystalline P(3HB), which is stated to be 149.37 J/g.[13] Although the degree of crystallinity determined using eq 1 cannot be treated as an absolute measure, the values can be used for relative comparison. The lab extracted P(3HB) was found to have a degree of crystallinity similar to that of the commercial P(3HB), as shown in Table 1.

3.2. Polymer and Composite Film Characterization. The surface morphology of polymer films produced using solvent casting is shown in Figure 3a, as observed by SEM. Solvent casting was used to prepare composites containing 5 and 20 wt % Bioglass particles. SEM analysis of the composite surface did not show the presence of a high concentration of Bioglass particles on the surface of the composite film, shown in Figure 3b,c. However, EDX analysis used to assess the distribution of Bioglass particles in the composite demonstrated the uniform distribution of Bioglass particles. The microstructure of composite sample cross sections was observed by SEM, as shown in Figure 3d. The image shows a fairly high density and relatively uniform thickness of the film.

Surface analysis was carried out using white light interferometry to visualize the topography of the composite film surfaces, as illustrated in Figure 3e,f. The surface roughness of the films does not change significantly with Bioglass addition: a typical rms (root-mean-square-average) value of 2.01 μm for neat polymeric films was found while 2.05 μm was the value for P(3HB)/20 wt % Bioglass films. This result is due to the fact that the Bioglass particles are being embedded in the polymer matrix. This feature of the present composites will have implications for their bioactive behavior as discussed below.

The effect of adding Bioglass particles on the molecular weight of the polymer was determined using GPC, and the results are shown in Table 2. Addition of Bioglass resulted in

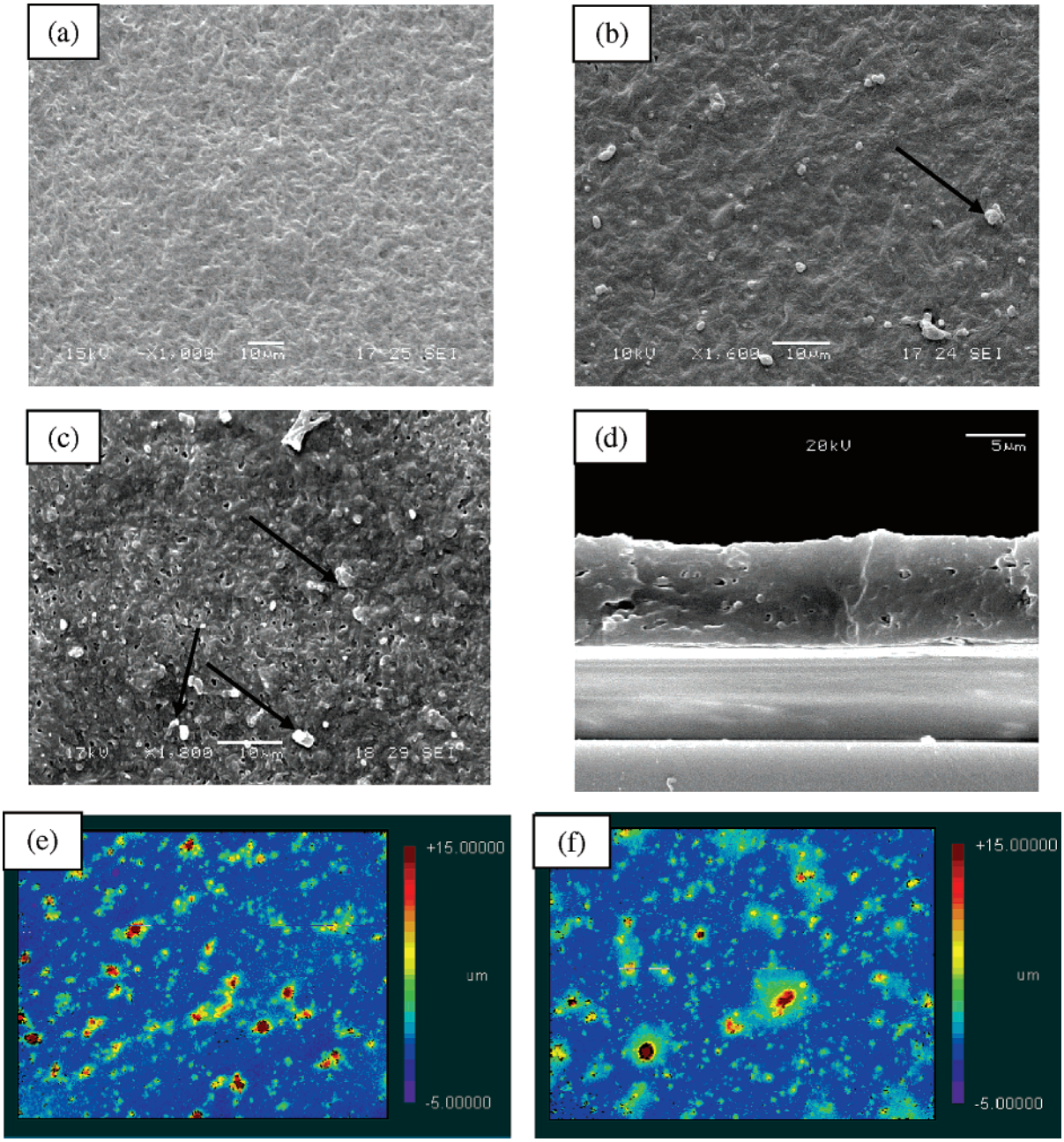

Figure 3. SEM images of (a) P(3HB) film, (b) P(3HB)/5 wt % Bioglass composite film, (c) P(3HB)/20 wt % Bioglass composite film, and (d) cross section of P3HB/20 wt % Bioglass composite film. The arrows in parts b and c indicate Bioglass particles. Surface topography analysis showing the surface profile and roughness for (e) P(3HB) film and (f) P(3HB)/20 wt % Bioglass composite, obtained by white light interferometry.

a slight decrease in the molecular weight of the polymer. Although addition of Bioglass particles resulted in a decrease of weight average molecular weight, the polydispersity index (PDI) remained the same, indicating a narrower spread of the molecular weight distribution.

Typical DSC thermograms of the polymer/Bioglass composite films are shown in Figure 4, which shows the first and second heating curves for the polymer and the composites. The absence of the prominent melting peak in the second heating for the composites as the Bioglass concentration increases from 5 to 20 wt % shows that the presence of Bioglass prohibits/retards the crystallization of the polymer. This phenomenon was not noticed for neat P(3HB), wherein the melting peaks were marked in the first and second heating cycle. Addition of Bioglass has also resulted in a reduction of the heat of fusion and hence a decrease of crystallinity for the composite, as shown in Table 2. Moreover, adding Bioglass also resulted in the emergence of two melting peaks during the first heating of the composites as shown in Figure 4.

Static tensile tests showed that the neat polymeric films achieved a Young's modulus of 1.1 ± 0.3 GPa. Addition of Bioglass led to a decrease in the Young's modulus of the composite, as shown in Table 2. The density of the composites was calculated using the rule of mixtures, and it was found to increase by the addition of Bioglass, as expected. DMA results were used to evaluate the viscoelastic properties (storage modulus, loss modulus, and tan δ) of polymer composites. The storage modulus and loss modulus were obtained in the temperature range −20 to 130 °C. The obtained results are plotted in Figure 5. The data plotted are typical plots obtained from the experiment, and a detailed set of data with standard deviation from the measurements is shown in Table 3. The

Table 2. Effect of Bioglass Concentration on Thermal Properties and Mechanical Properties[a]

property	0 wt %	5 wt %	20 wt %
vol %[c]	0	2.2	8.44
T_m (°C)	172 ± 2	152/169[b]	156/172[b]
ΔH_f (J/g)	0.49	0.41	0.40
X_c (%)	73 ± 1	60 ± 4	60 ± 2
M_w[d]	285000	245000	261000
PDI[e]	2.6	2.7	2.5
Tg[f] (°C)	−6.3 ± 0.6	−5 ± 3	−1.2 ± 0.5
ρ_c[g]	1.12	1.23	1.32
E[h] (GPa)	1.1 ± 0.3	0.8 ± 0.1	0.84 ± 0.05
H[i] (GPa)	0.12 ± 0.02		0.18 ± 0.09

[a] Thermal data for the composites were recorded from the first heating cycle of DSC runs. [b] Denotes the presence of primary and secondary melting peaks. [c] Vol % = volume percent of Bioglass. [d] M_w = weight average molecular weight. [e] PDI = polydispersity index. [f] Tg = glass transition temperature calculated from DMA. [g] ρ_c = density of composite. [h] E = Young's modulus. [i] H = hardness calculated from nanoindentation.

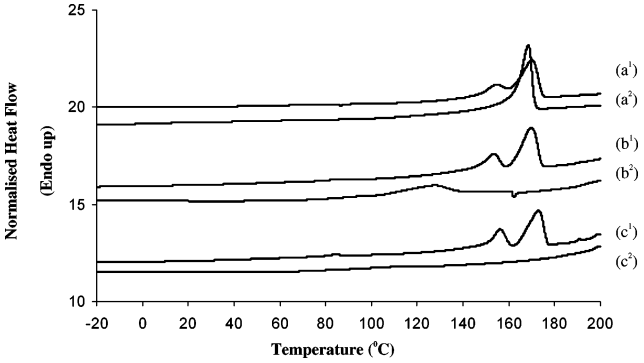

Figure 4. First (1) and second (2) normalized heating DSC curves of (a) P(3HB), (b) P(3HB)/5 wt % Bioglass, and (c) P(3HB)/20 wt % Bioglass samples. The units of the *y*-axis are arbitrary, and curves are shifted vertically for clarity.

storage modulus was found to increase for P(3HB) composites containing 20 wt % Bioglass particles. It was also noted that the storage modulus decreased with the increase in temperature. T_g-P(3HB) (glass transition temperature defined as the temperature where the loss modulus obtained its peak value) and tan δ measurement results are shown in Tables 2 and 3, respectively. It can be deduced that the addition of Bioglass increased the glass transition temperature of the polymer.

Nanoindentation tests carried out on polymer films also showed a Young's modulus for the neat polymeric film to be on the order of 1.1 ± 0.1 GPa (in excellent agreement with static tensile tests). Nanoindentation analysis of the polymer composites showed the hardness of the composite to increase due to the addition of Bioglass (Table 2), as expected.

3.3. In vitro Bioactivity Results in Simulated Body Fluid. P(3HB)/Bioglass composite films were immersed in SBF to identify the potential bioactivity induced by the presence of Bioglass. This effect was determined by analyzing the possible formation of a layer of hydroxyapatite (HA) on the sample surfaces as is common practice in the biomaterials field.[27,28,34] The formation of hydroxyapatite crystals localized on the Bioglass particles was confirmed by SEM after 7 days of immersion in SBF, as shown in Figure 6a,b. Extensive formation of hydroxyapatite crystals, forming a continuous layer, was observed on the surface of the composites after 28 days of immersion time. XRD results as shown in Figure 6c confirm the formation of weakly crystalline HA on composite surfaces after only 7 days of immersion in SBF, which verifies the potential high bioactivity of the present composites.

4. Discussion

4.1. Polymer Characterization. The results of thermal and molecular analyses on the laboratory grown polymer (extracted from *Bacillus cereus* SPV) were found to be closely similar to those reported in the literature.[11] Further comparison of the lab grown P(3HB) with the commercially available P(3HB) showed that the polymers have similar X-ray diffraction patterns (Figure 1). Moreover, the crystallization temperature, heat of fusion, and glass transition temperature for both polymers were found to be similar, except for the melting temperature. The lab grown P(3HB) was found to have a lower melting temperature than the commercial P(3HB). Although P(3HB) is bacterially produced, it is known to have a range of properties due to the differences in the organism used and the production process. Therefore, it is in our interest to determine the thermal properties of the lab polymer and compare it with the commercially available P(3HB). It was also found that 6−8 wt % of the lab grown P(3HB) can be easily dissolved in chloroform at room temperature, which is not the case for commercial P(3HB). In addition to extracting a polymer with consistent thermal and molecular data, it was also possible to extract the polymer with a crystallinity percentage very near to its possible lowest value of 46%.[6−11] However, the crystallinity of the polymer greatly depends on the type of extraction process used. For example, there are certain methods that have led to extraction of amorphous P(3HB) by using enzymatic extraction techniques.[36] The Young's modulus of the biopolymers determined by the static tensile test and nanoindentation was 1.1 GPa. Although the Young's modulus of P(3HB) has been reported to be in the range of 3−5 GPa,[11,14] the values for polymeric films obtained by solvent casting technique tend to be lower and in fact similar to the values reported in the literature for P(3HB) films.[37] To the authors' knowledge, the present investigation is the first to report mechanical, structural, and thermal properties of P(3HB) extracted from *Bacillus cereus* SPV and to have used this polymer for formation of composites with 45S5 Bioglass particles.

4.2. Bioglass Particle Distribution in Composite Films. The uniform distribution of Bioglass particles is important for homogeneous growth of a hydroxyapatite (HA) layer upon immersion of the samples in simulated body fluid (SBF). In this experiment, it was possible to disperse the Bioglass particles uniformly by sonicating the P(3HB)/Bioglass suspension. Bioglass particles were, however, not present at large on the surfaces of the films; instead, they were embedded in the polymer matrix. This fact was further established by SEM observations, surface analysis, and the bioactivity results in SBF. It is suggested that this may be the reason why addition of Bioglass particles did not significantly increase the surface roughness of the films as shown in Figure 3e,f. The relatively slower degradation of the polymer surface (52 weeks)[11,15] upon immersion in SBF would lead to a progressive exposure of the Bioglass particles with a time dependent increase of bioactivity.

4.3. Effect of Bioglass Addition on Properties of P(3HB) Films. Bioglass is known to influence the properties of polymer matrix composites by altering the thermal, mechanical, and degradation properties.[4,28,30] Similar conclusions can be drawn from our experimental results, wherein the thermal and mechanical properties of the composite were found to change due to the addition of Bioglass. The presence of Bioglass particles in the P(3HB) affected the thermal properties of the composites, as shown in Figure 4 and Table 2. The absence of the melting peaks during the second heating run for the 20 wt % composite denotes that the presence of Bioglass in the polymer actually

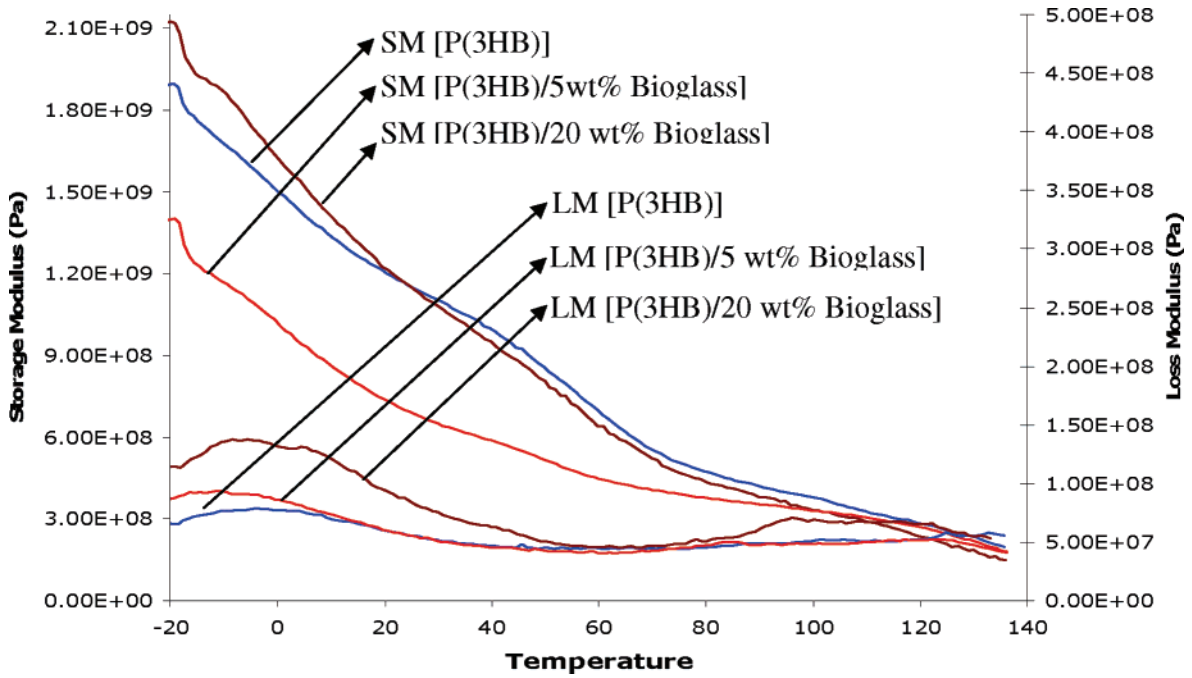

Figure 5. Typical plot of storage modulus (SM) and loss modulus (LM) against temperature for P(3HB), P(3HB)/5 wt % Bioglass, and P(3HB)/20 wt % Bioglass composites.

Table 3. Mean and Standard Deviation of Storage Modulus (E'), Loss Modulus (E''), and Tan δ for Bioglass Reinforced P(3HB) Composites at Various Temperatures

	Bioglass content (wt %)	−20 °C	0 °C	20 °C	50 °C
storage modulus (units 10^9 Pa)	0	2.1 ± 0.3	1.6 ± 0.1	1.3 ± 0.1	0.90 ± 0.04
	5	1.4 ± 0.2	1.0 ± 0.1	0.8 ± 0.1	0.6 ± 0.1
	20	2.4 ± 0.6	1.8 ± 0.3	1.4 ± 0.3	0.9 ± 0.2
loss modulus (units 10^7 Pa)	0	9 ± 3	9 ± 2	7 ± 1	5.3 ± 0.7
	5	10 ± 1	10 ± 2	8 ± 2	6 ± 2
	20	16 ± 5	18 ± 4	13 ± 5	6 ± 1
tan δ	0	0.04 ± 0.01	0.06 ± 0.01	0.05 ± 0.01	0.88 ± 0.04
	5	0.07 ± 0.01	0.1 ± 0.02	0.1 ± 0.02	0.11 ± 0.02
	20	0.06 ± 0.01	0.09 ± 0.03	0.09 ± 0.03	0.11 ± 0.06

retards the possible crystallization of the polymer from the melt, due to the heating up to 200 °C during the first run. However, for a lower Bioglass content of 5 wt % there was evidence of a small melting peak during the second heating run, indicating that the polymer is able to recrystallize after the first heating cycle. This can in turn have an effect on the degradation temperature of the composite system. For example, addition of hydroxyapatite to the polymer matrix of poly(hydroxybutyrate-*co*-hydroxyvalerate) considerably reduces the degradation temperature as shown in the literature.[23] Such an effect of Bioglass on the composite can pose problems when using heat processing techniques to prepare P(3HB)/Bioglass composites, e.g., extrusion or sintering. The emergence of a prominent secondary melting peak during the first heating for the composite samples (Figure 4) suggests that addition of Bioglass may cause the formation of primary crystals which melt at a lower temperature. In addition to inducing the growth of primary crystals, the presence of high concentration of Bioglass can also hinder the growth of these crystallites in the polymer; consequently, the degree of crystallinity for the composite decreases. This can be seen from Table 2, wherein the degree of crystallinity is reduced by increasing the Bioglass content. The consequence of this lowered crystallinity would aid in increasing the rate of in vivo degradation of the polymer, which is known to have a relative long period of degradation time (52 weeks).[6−11] Static tensile tests showed that the inclusion of Bioglass particles reduces the Young's modulus of the composites. Such a decrease in the modulus on increasing the filler content may be due to the dewetting effect through which the adhesion strength between the filler and the matrix phases is decreased or even suppressed. The dewetting also reduces the surface area in contact with the filler, which reduces the filler's efficiency in enhancing the modulus.[38] Another reason for a decrease in the modulus of the composite may be the possible presence of some Bioglass particle agglomerations. Agglomerates act as weak points in the material and break easily when stress is applied.[39] Broken agglomerates then act as stress concentrators leading to microcracking, effectively decreasing the modulus of the composites.[38]

DMA has been used to extensively characterize particulate reinforced polymer composites.[23,38−40] P(3HB), being a viscoelastic polymer, stores mechanical energy without dissipation of it (measured as storage modulus E'), and also dissipates energy on deformation (measured as loss modulus E''). In a polymer−matrix composite, the energy dissipation may also come from the filler−matrix interface where friction between the two phases occurs. The internal friction can be quantified by tan δ, which is the ratio of the energy dissipated per cycle to the energy stored during the cycle. The three important

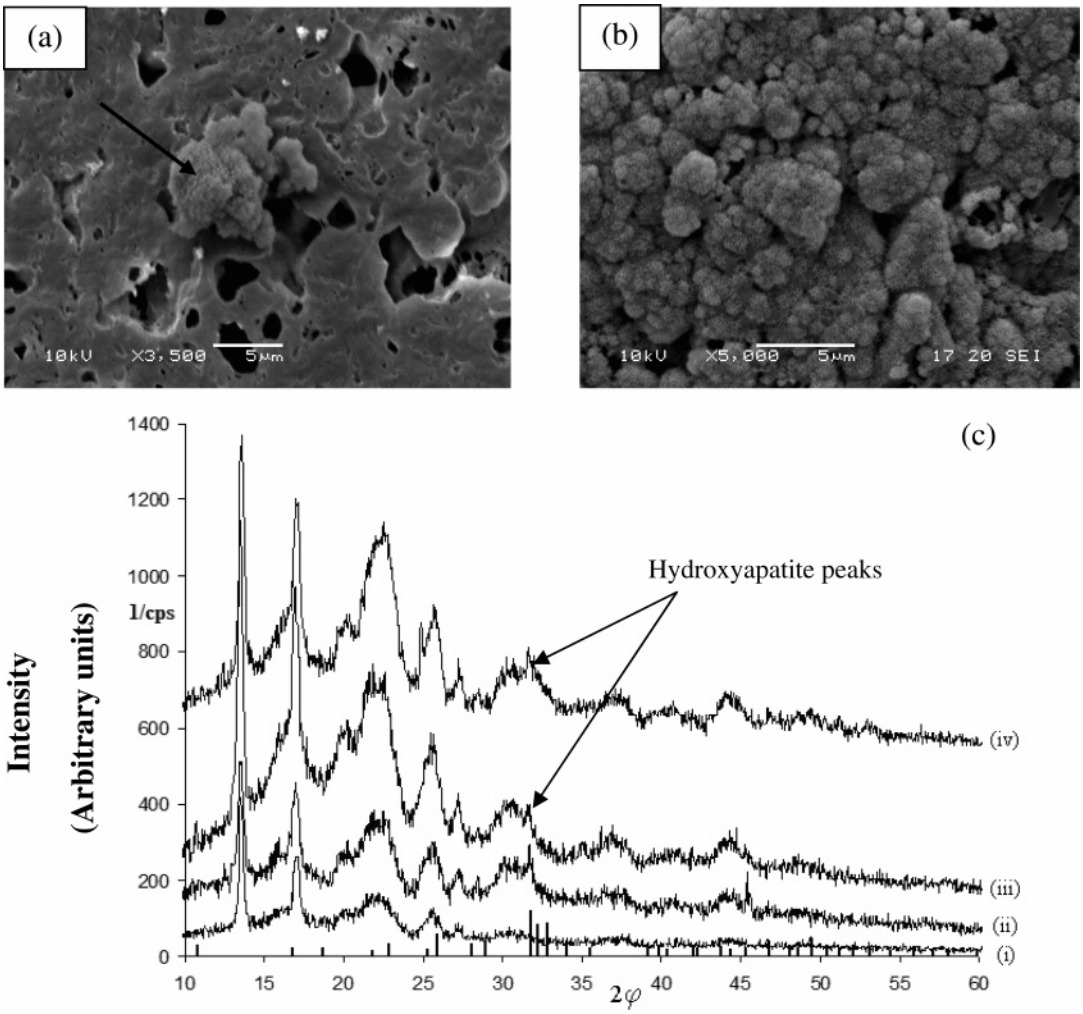

Figure 6. SEM images of P(3HB)/Bioglass composite (20 wt % of Bioglass) immersed in SBF for (a) 7 days, the arrow indicates the formation of hydroxyapatite crystals, and (b) 1 month, showing the extensive growth of hydroxyapatite crystals forming a continuous layer on the surface of the composites. The X-ray diffraction patterns of in vitro degraded P(3HB)/Bioglass composites (20 wt %), after immersion in SBF as shown in part c for (i) 0 days, (ii) 2 days, (iii) 7 days, and (iv) 28 days.

observations made from the DMA analysis on the present materials are described as follows. First, the increase in Bioglass concentration effectively increases the T_g of the polymer, as can be seen in Table 2. It is possible that the T_g increase was due to the partial immobilization of the polymer chains and the physical blocking of a number of molecular configurations as a result of adsorption onto the filler surface. However, there have been reports wherein an increase in the T_g occurs when the adhesion between the polymer and the filler has been suppressed.[38] Second, the increase in Bioglass content also results in an increase in tan δ; in other words, the damping capacity of the material is increased. Such behavior can occur due to the introduction of new damping mechanisms that are not present in the neat polymer. Some of the possible explanations for this increase are the following: (a) Bioglass−Bioglass particle friction where particles touch one another as in weak agglomerates, (b) P(3HB)−Bioglass friction where there is essentially no adhesion at the interface, and (c) excess damping in the polymer near the interface because of induced thermal stresses or changes in polymer conformation or morphology. Finally, the storage modulus was found to increase by the addition of 20 wt % Bioglass; however, on increasing the temperature the storage modulus was found to have a similar value compared to the neat P(3HB) samples. This further cements the previous observation that there might be a weak polymer/ Bioglass interfacial strength.

The hardness of the composite was improved due to the addition of Bioglass. The Young's modulus of the polymer films predicted by the nanoindentation technique was found to be very similar to the values found by the static tensile tests. However, a relatively higher Young's modulus value was recorded for the composites (data not shown). This behavior shows that the technique is not appropriate to determine the Young's modulus in this type of composite. Increase in the hardness of the composites due to Bioglass incorporation makes them suitable for hard tissue applications or coatings of implants where strength and hardness are of vital importance. Further tests are being carried out to understand the interaction between P(3HB) and Bioglass and the effect of tailoring interfaces using surface treated Bioglass particles.

4.4. Bioactivity of P(3HB)/Bioglass Composites. In addition to altering mechanical properties, the incorporation of Bioglass particulates in the polymer matrix promotes the formation of hydroxyapatite in contact with simulated body fluid. The formation of HA occurs from the surface of Bioglass particles by a well-known mechanism;[27] hence, it is important that Bioglass particles are exposed to the fluid environment at various stages during in vitro degradation of the composite. In this study, formation of HA crystals on film surfaces was possible after only 7 days of immersion in SBF (Figure 6). However, the lack of prominent HA peaks in the X-ray diffractogram emerging after immersion of composites in SBF may be due to the follow-

ing: (i) the majority of the Bioglass particles were embedded in the polymer matrix preventing direct contact with SBF, hence a longer immersion time in SBF would be required, or (ii) the HA peaks overlapped with the crystalline peaks of the polymer, and a weakly crystalline nature of the layer formed. However, the former reason is more likely. It is also possible that the HA formed is not stoichiometric (e.g., Ca/P ratio <1.6) in agreement with previous investigations where HA has been precipitated on Bioglass containing composites from SBF.[28,30] The results would indicate that the composite exhibits an initial HA formation stage (as shown in Figure 6) followed by gradual increase in HA formation. In an in vivo situation, as more Bioglass particles come in contact with body fluid with increasing immersion time, there will be a consequent gradual increase in the interfacial strength between the composite and the surrounding tissues due to increased formation of HA. The exposure of the Bioglass particles will depend on the degradation rate of the polymer. Yamane et al.[41] have shown that the degradation of this polymer is a function of the crystallinity and especially of the highly ordered β-crystalline parts of the structure. Therefore, a longer immersion period of the polymer in SBF or longer period of implantation will result in the breakdown of the polymer matrix and increase in the exposure of the Bioglass particles leading to high degree of HA formation (higher bioactivity).

5. Conclusions

The thermal and structural properties of the extracted polymer were found to have similar values when compared to the commercially available P(3HB). However, a higher concentration (6−8 wt %) of polymer is easily dissolved in chloroform at room temperature compared to the commercial P(3HB) that needs to be heated; thus, the polymer synthesized in this work has better processibility for composite preparation. P(3HB)/Bioglass composite production through solvent casting was demonstrated to yield homogeneous composite microstructure. The presence of Bioglass led to a reduction in the crystallinity of the polymer along with an increase in the hardness of the composite. However, the Young's modulus of the composite deteriorated with addition of Bioglass, possibly due to the lack of interfacial strength between the polymer and the Bioglass particles. The damping of the composite was also found to increase along with the polymer glass transition temperature on increasing Bioglass content. Further tests are needed to effectively understand the interaction between Bioglass and the polymeric matrix. Ways of improving the interfacial strength between the Bioglass particles and the polymer matrix will be investigated in further studies. Moreover, research on PHA/Bioglass composites will be directed toward optimizing the composite's mechanical properties and tailoring the degradation rate, with focus on understanding how the addition of Bioglass can be used to alter the degradation rate of the polymer.

Acknowledgment. The authors would like to thank EPSRC (EP/C515617/1, U.K.) and Overseas Research Scholarships (U.K.) for financial assistance. Dr. S. Holding and the group at RAPRA Ltd, U.K., are acknowledged for carrying out the molecular mass measurements. Special thanks to Ms. Qizhi Chen for her support with SBF work.

References and Notes

(1) Braddock, M.; Houston, P.; Campbell, C.; Ashcroft, P. *News Physiol. Sci.* **2001**, *16*, 208.
(2) Goldberg, V. M.; Stevenson, S. *Clin. Orthop.* **1987**, *225*, 7.
(3) Bonfiglio, M.; Jeter, W. S. *Clin. Orthop.* **1972**, *87*, 19.
(4) Khademhosseini, A.; Langer, R.; Borenstein, J.; Vacanti, J. P. *Proc. Natl. Acad Sci. U.S.A.* **2006**, *103*, 2480.
(5) Langer, R.; Vacanti, J. P. *Science* **1993**, *260*, 920.
(6) Williams, S. F.; Martin, D. P.;. Horowitz, D. M.; Peoples, O. P. *Int. J. Biol. Macromol.* **1999**, *25*, 111.
(7) Yang, S.; Leong, K.; Du, Z.; Chua, C. *Tissue Eng.* **2001**, *7*, 679.
(8) Wu, L. *Tissue Eng.* **2005**, *11*, 264.
(9) Kohn, J.; Abramson, S.; Langer, R. In *Biomaterials Science*—An Introduction to Materials in Medicine, 2nd ed.; Ratner, B. D., Hoffman, A. S., Schoen, F. J., Lemons, J. L., Eds.; Elsevier Academic Press: London, 2006; Chapter 2.
(10) Steinbüchel, A. *Macromol. Biosci.* **2001**, *1*, 1.
(11) *Biopolymers Volume 4*—Polyesters III; Doi, Y., Steinbüchel, A., Eds.; Wiley-VCH: Weinheim, 2001; pp 53−129.
(12) Luklinska, Z. B.; Bonfield, W. *J. Mater. Sci.: Mater Med.* **1997**, *8*, 379.
(13) Doyle, C.; Tanner, E. T.; Bonfield, W. *Biomaterials* **1991**, *12*, 841.
(14) Misra, S. K.; Valappil, S. P.; Roy, I.; Boccaccini, A. R. *Biomacromolecules* **2006**, *7*, 2249.
(15) Anderson, A. J.; Dawes, E. A. *Microbiol. Rev.* **1990**, *54*, 450.
(16) Fukada, E.; Ando, Y. *Int. J. Biol. Macromol.* **1986**, *8*, 361.
(17) Reusch, R. N. *Can. J. Microbiol.* **1995**, *41*, 50.
(18) Luklinska, Z. B.; Schluckwerder, H. *J. Microsc. (Oxford)* **2003**, *211*, 121.
(19) Shishatskaya, E. I.; Volova, T. G. *J. Mater. Sci.: Mater. Med.* **2004**, *15*, 915.
(20) Shishatskaya, E. I.; Volova, T. G.; Puzyr, A. P.; Mogilnaya, O. A. *J. Mater. Sci.: Mater. Med.* **2004**, *15*, 719.
(21) Gogowleski, S.; Jovanovic, M.; Perren, S. M.; Dillon, J. G.; Hughes, M. K. *J. Biomed. Mater. Res.* **1993**, *27*, 1135.
(22) Knowles, J. C.; Hastings, G. W.; Ohta, H.; Niwa, S.; Boeree, N. *Biomaterials* **1992**, *13*, 491.
(23) Chen, L. J.; Wang, M. *Biomaterials* **2002**, *23*, 2631.
(24) Li, H.; Chang, J. *Biomaterials* **2004**, *25*, 5473.
(25) Rezwan, K.; Chen, Q. Z.; Blaker, J. J.; Boccaccini, A. R. *Biomaterials* **2006**, *27*, 3413.
(26) *Introduction to Bioceramics*; Hench, L. L., Wilson, J., Eds.; Singapore World Scientific: Singapore, 1993.
(27) Hench, L. L. *J. Am. Ceram. Soc.* **1998**, *81*, 1705.
(28) Boccaccini, A. R.; Maquet, V. *Compos. Sci. Technol.* **2003**, *63*, 2417.
(29) Xynos, I. D.; Edgar, A. J.; Buttery, L. D. K.; Hench, L. L.; Polak, M. *J. Biomed. Mater. Res.* **2001**, *55*, 151.
(30) Roether, J. A.; Boccaccini, A. R.; Hench, L. L.; Maquet, V.; Gautier, S.; Jérôme, R. *Biomaterials* **2002**, *23*, 3871.
(31) Valappil, S. P.; Perris, D.; Langley, G. L.; Herniman, J. M.; Boccaccini, A. R.; Bucke, I. R.; Roy, I. *J. Biotechnol.* **2007**, *127*, 475.
(32) Kannan, L. V.; Rehacek, Z. *Indian J. Biochem.* **1970**, *7*, 126.
(33) Ramsay, J. A.; Berger, E.; Voyer, R.; Chavarie, C.; Ramsay, B. A. *Biotechnol. Tech.* **1994**, *8*, 589.
(34) Kokubo, T.; Kushitani, H.; Sakka, S.; Kitsugi, T.; Yamamuro, T. *J. Biomed. Mater. Res.* **1990**, *24*, 721.
(35) Skrbic, Z.; Divjakovic, V. *Polymer* **1996**, *37*, 505.
(36) Holmes, P. A.; Lim, G. B. U.S. Patent 4, 910,145, 1990.
(37) Aoyagi, Y.; Doi, Y.; Iwata, T. *Polym. Degrad. Stab.* **2003**, *79*, 209.
(38) Nielsen, L. E.; Landel, R. F. In *Mechanical Properties of Polymers and Composites*, 2nd ed.; Nielsen, L. E., Landel, R. F., Eds.; Marcel Dekker Inc.: New York, 1994; Chapter 7.
(39) Bleach, N. C.; Nazhat, S. N.; Tanner, K. E.; Kellomäki, M.; Törmälä, P. *Biomaterials* **2002**, *23*, 1579.
(40) Nazhat S. N.; Kellomäki, M.; Törmälä, P.; Tanner, K. E.; Bonfield, W. *J. Biomed. Mater. Res.* 2**001**, *58*, 335.
(41) Yamane, H.; Terao, K.; Hiki, S.; Kawahara, Y.; Kimura, Y.; Saito, T. *Polymer* **2001**, *42*, 7873.

BM0701954